miR-196a downregulation increases the expression of type I and III collagens in keloid fibroblasts

Kazuya Kashiyama[1, 3], Norisato Mitsutake[1, 6], Michiko Matsuse[1], Tomoo Ogi[1, 6], Vladimir Saenko[2], Kenta Ujifuku[4], Atsushi Utani[5], Akiyoshi Hirano[3] and Shunichi Yamashita[1, 2]

[1]Department of Radiation Medical Sciences, Atomic Bomb Disease Institute, Nagasaki University Graduate School of Biomedical Sciences, Nagasaki, Japan

[2]Department of Health Risk Control, Atomic Bomb Disease Institute, Nagasaki University Graduate School of Biomedical Sciences, Nagasaki, Japan

[3]Division of Plastic and Reconstructive Surgery, Department of Developmental and Reconstructive Medicine, Nagasaki University Graduate School of Biomedical Sciences, Nagasaki, Japan

[4]Department of Neurosurgery, Nagasaki University Graduate School of Biomedical Sciences, Nagasaki, Japan

[5]Department of Dermatology, Nagasaki University Graduate School of Biomedical Sciences, Nagasaki, Japan

[6]Nagasaki University Research Centre for Genomic Instability and Carcinogenesis (NRGIC), Nagasaki, Japan

Short Title: miR-196a and collagen I&III in keloids

Corresponding author: Norisato Mitsutake, MD PhD

Department of Radiation Medical Sciences, Atomic Bomb Disease Institute, Nagasaki University Graduate School of Biomedical Sciences

1-12-4 Sakamoto, Nagasaki 852-8523, Japan

Tel: +81 (95) 849-7116, Fax: +81 (95) 849-7117

E-mail: mitsu@nagasaki-u.ac.jp

Abstract

Keloids are a fibroproliferative disease due to abnormal wound healing process after skin injury. They are characterized by over-production of extracellular matrix (ECM) such as collagens. MicroRNAs (miRNAs) are non-coding small RNAs and negatively regulate protein expression. Several miRNAs that play critical roles in tissue fibrosis and ECM metabolism have been reported. However, regulation and function of miRNAs in keloid remain to be explored. The purpose of the present study was to identify miRNAs involved in keloid pathogenesis. We performed miRNA microarray analysis to compare miRNA expression profiles between keloid-derived fibroblasts (KF) and normal fibroblasts (NF). Seven upregulated and twenty downregulated miRNAs were identified. Among these, we focused on miR-196a, which showed the highest fold-change. Overexpression or knockdown of miR-196a led to a decreased or increased level of secreted type I/III collagens, respectively. Reporter analysis showed direct binding of miR-196a to the 3'UTR of *COL1A1* and *COL3A1*. In conclusion, we demonstrate for the first time that miRNA expression profile is altered in KF compared with NF. Downregulation of miR-196a may be one of the mechanisms by which collagens are highly deposited in keloid tissues. Our findings suggest that miR-196a could be a novel therapeutic target for keloid lesion.

Introduction

Keloids are a benign dermal fibroproliferative disease due to abnormal wound healing process after skin injury. They are characterized by over-production of extracellular matrix (ECM) and invasiveness beyond the original boundary of the insult. Excess deposition of ECM such as collagen (Niessen *et al.*, 1999; Syed *et al.*, 2011) by fibroblasts is responsible for keloid, but its etiology and mechanism are still poorly understood. Although keloid is a benign dermal tumor, its management is one of the most challenging clinical problems. Keloids do not regress with time, and surgical excision alone results in a high rate of recurrence. Various conservative therapies have been attempted, but definite and effective treatment has not been established yet (Al-Attar *et al.*, 2006; Seifert and Mrowietz, 2009).

MicroRNAs (miRNAs) are non-coding and single-stranded small RNAs that negatively regulate gene expression. Mature miRNA is approximately 22 nucleotides in length; it binds to target messenger RNA (mRNA) and induces its cleavage or translational repression depending on the degree of complementarity (Bartel, 2004). miRNAs play critical roles in many important biological processes, such as cell growth, proliferation, differentiation and apoptosis (Esquela-Kerscher and Slack, 2006). To date, hundreds of miRNAs have been identified to be dysregulated in various diseased tissues (Lu *et al.*, 2008), but only a fraction of them has been functionally characterized.

Recently, some miRNAs have been reported to participate in fibrosis and ECM metabolism (Chau and Brenner, 2011; Jiang *et al.*, 2010). The miR-29 family members (miR-29a, miR-29b, miR-29c) directly regulate translation of various ECM mRNAs, such as collagen superfamily (Chau and Brenner, 2011; Jiang *et al.*, 2010). They are also implicated in fibroblasts in cardiac fibrosis (van Rooij *et al.*, 2008), stellate cells in hepatic fibrosis

(Ogawa *et al.*, 2010; Roderburg *et al.*, 2011) and dermal fibroblasts in systemic sclerosis (Maurer *et al.*, 2010). miR-21 expression is increased selectively in fibroblasts in failing heart and controls interstitial fibrosis and cardiac hypertrophy (Thum *et al.*, 2008).

As a novel therapeutic approach for fibrotic disorders, several miRNA gene therapies have been attempted. In particular, antagonizing endogenously upregulated miRNA using antisense strand has been proposed (Brown and Naldini, 2009). Van Rooij et al. showed that inhibiting miR-29 using cholesterol-conjugated antisense strand increased collagen expression in mice liver, kidney and heart (van Rooij *et al.*, 2008). Another group reported that inhibition of miR-21 prevented interstitial fibrosis and cardiac hypertrophy in a mouse model of heart infarction (Thum *et al.*, 2011).

Thus, miRNAs play a number of roles in fibrosis and have attracted attention as a novel target for gene therapy. However, regulation and function of miRNAs in keloid tissues remain unknown. In the present study, we performed a comprehensive analysis of miRNA expression in keloid-derived fibroblasts (KF) and normal fibroblasts (NF) using miRNA microarray and then explored the function of miR-196a, which showed the highest fold-change in KF compared with NF.

Results and Discussion

Expression profile of miRNAs in KF

To identify miRNAs specifically regulated in KF, we first performed a comprehensive analysis of miRNA expression in KF and NF using miRNA expression microarrays. Each three samples of KF and NF were examined for changes in miRNA expression (Table 1).

Twenty seven miRNAs were identified to be differentially expressed in KF compared with NF (unpaired t-test, $p<0.05$): seven miRNAs were overexpressed, and 20 were underexpressed (Table 2). Among these miRNAs, miRNA-142-3p and miR-196a showed the highest fold-change (miR-142-3p: 9.856-fold and miR-196a: 0.093-fold in KF compared with NF). Then we focused on these two miRNAs in the following analysis.

Comparative analysis of the miRNA expression at passage 0 and 2

Change of gene expressions and growth factor kinetics due to passage and/or long time culture have become an important problem in *in vitro* research using primary fibroblasts (Hirth *et al.*, 2002; Yuan *et al.*, 1996). Therefore, we first compared the expression of those miRNAs in primary fibroblasts at passage 0 with that at passage 2 by TaqMan real-time RT-PCR assay. Surprisingly, the apparent difference in miR-142-3p expression at passage 0 was completely lost at passage 2 (Figure 1a). By contrast, the difference in miR-196a tended to be expanded after passage 2 (Figure 1b). These data suggest that miRNA expression could be rapidly altered during early passages. In general, primary fibroblasts with low passage number are used to compare gene expression to avoid loss of characteristics (Feghali and Wright, 1999; Seifert *et al.*, 2008; Smith *et al.*, 2008). It has been reported that collagen gene expression changed gradually during passage 0-3 in primary KF (Syed *et al.*, 2011). Similarly, the expression pattern of integrin collagen receptors changed in KF at successive passages 0-4 (Szulgit *et al.*, 2002). Likewise, the effect of passage and milieu alteration may affect miRNA expression in KF. According to our results (Figure 1), the degree of change seems to be dependent on each individual miRNA, suggesting that careful analysis is required in experiment to measure a miRNA expression level in primary KF. Hence, KF and NF at passage 0 were used in the following experiments.

Validation of the miRNA expression by real-time RT-PCR

To validate the microarray data, we also performed the TaqMan real-time RT-PCR assay for miR-142-3p and miR-196a in KF and NF using nine samples each (Table 1). As shown in Figure 2, miR-142-3p was overexpressed (Figure 2a) and miR-196a was underexpressed (Figure 2b) in KF compared with NF, and these differences were statistically significant. Of nine keloid samples, KF1 and KF4 were obtained from different sites, chest and shoulder, in a same patient. Six were caused by minor wounds such as acne and scratch, and three were by surgical operations: lung cancer, coronary artery bypass grafting and recurrence of keloid resected 20 years ago (Table 1). Six cases had previous treatments such as topical corticosteroid and oral administration of Tranilast, but they were ineffective (Table 1). There seems to be no correlation between the miRNA expression level and clinical features. These data indicate that we successfully confirmed the differential expressions of miR-142-3p and miR-196a in KF and NF.

***In silico* identification of possible target genes**

To explore the mechanisms by which these miRNAs contribute to keloid pathogenesis, three web-based databases, miRanda (Betel *et al.*, 2008), TargetScan (Lewis *et al.*, 2005) and PicTar (Krek *et al.*, 2005) were used to search for possible target mRNAs of these miRNAs. Regarding targets of miR142-3p, 2,634 genes in miRanda, 250 genes in TargetScan and 200 genes in PicTar were predicted. Among the three databases, 70 genes were commonly shared (Figure S1) and are listed in Table S1. Correspondingly, 47 genes were shared as targets of miR-196a (Table S2): 2,783 genes in miRanda, 180 genes in TargetScan and 162 genes in PicTar (Figure S1).

Collagen genes as a target of miR-196a

miRNAs were initially proposed to mediate translational repression of their target mRNAs. However, it has been recently demonstrated that this is often accompanied by decrease in mRNA abundance itself (Baek *et al.*, 2008; Selbach *et al.*, 2008). We therefore searched for target genes of miR-142-3p using real-time RT-PCR for mRNA; among the candidate genes, we examined *ADCY9*, *BCLAF1*, *CFL2*, *COL24A1*, *HMGA2* and *ROCK2*, which are implicated in collagen synthesis, apoptosis, actin filaments, collagen, TGFβ signaling and Rho-actin signaling, respectively. Unfortunately, we did not identify reproducible differences in any of these candidates between nine KF and nine NF samples (data not shown). Presumably, these genes are regulated by a number of different pathways, and miR-142-3p is probably not a major effector in dermal fibroblasts.

Among the predicted target genes of miR-196a, we focused on collagens (*COL1A1*, *COL1A2*, *COL3A1*), because one of the major findings in keloid pathology is increased ECM deposition, and collagen family is a dominant component of ECM (Al-Attar *et al.*, 2006). The expression of some of collagen mRNAs is increased in KF (Shih and Bayat, 2010), and type I and III collagen proteins are increased in keloid (Ala-Kokko *et al.*, 1987; Syed *et al.*, 2011). We confirmed the increased level of *COL1A1*, *COL1A2* and *COL3A1* mRNAs in our samples (Figure S2).

Indeed, *COL1A1*, *COL1A2* and *COL3A1* have potential miR-196a target site in their 3'UTR, and the complementarity between the target sites and the miR-196a seed region (2-8 nucleotides of the 5'-end of miR-196a) is completely matched (Figure S3). The complementarity between the seed region of miRNA and 3'UTR of mRNAs is the most important determinant for target specificity (Bartel, 2009), and miRNA-mediated translational repression often depends on perfect or near-perfect base pairing of a seed region to its target (Doench and Sharp, 2004). Therefore, type I and III collagens are strong

candidates that are regulated by miR-196a.

Effect of miR-196a on the expression of collagens

To determine the biological function of miR-196a, we used predesigned and functionally tested Pre-miR™ miRNA Precursor Molecule (Pre-miR-196a) and Anti-miR™ miRNA Inhibitor (Anti-miR-196a) to overexpress and knockdown miR-196a, respectively. We first assessed transfection efficiency using FAM-labeled Pre-miR™ and Anti-miR™ Scrambled Negative Control (Scrambled) with a fluorescence microscope, and it was almost 100% in our hands (data not shown). We also confirmed a robust increase of the miR-196a level following Pre-miR-196a transfection (Figure 3a) by TaqMan real-time RT-PCR assay. We then transfected NF and KF with Pre-miR-196a or Anti-miR-196a, and the protein levels of collagens secreted into supernatants were measured by western blot. The secretion of type I and III collagens into culture media was reduced in KF and NF transfected with Pre-miR-196a (Figure 3b). On the other hand, knockdown of miR-196a by Anti-miR-196a increased the expression of those collagens (Figure 3b). These results suggest that miR-196a regulates the secretion of collagen I and III in fibroblasts of dermal tissue.

Luciferase reporter assay

To further investigate whether miR-196a directly regulates the expression of type I and III collagens, we generated luciferase reporter plasmids containing the 3'UTR of the *COL1A1* or *COL3A1* gene (pmirGLO-COL1A1-3'UTR and pmirGLO-COL3A1-3'UTR). First, we transfected these plasmids into NF and KF and measured luciferase activity. As shown in Figure 3c, the luciferase activity in KF was significantly higher than that in NF. It may reflect the difference of the miR-196a expression between KF and NF. Next, NF were transfected wtih the reporter plasmids together with Pre-miR-196a or Anti-miR-196a. As

shown in Figure 3d, cotransfection with Pre-miR-196a reduced both luciferase activities driven from the reporter plasmids carrying the *COL1A1* and *COL3A1* 3'UTR. Moreover, Anti-miR-196a increased the luciferase activities as compared with the scramble (Figure 3e). These findings suggest that miR-196a directly regulates the expression of collagen I and III through targeting the 3'UTRs of the *COL1A1* and *COL3A1* genes in fibroblasts.

CpG island methylation of the miR-196a promoters.

It has been recently reported that some of disease-associated miRNAs are silenced by aberrant DNA methylation of their promoter CpG island (Bandres *et al.*, 2009; Kozaki *et al.*, 2008; Lujambio *et al.*, 2007; Tsai *et al.*, 2010). To determine whether promoter methylation is responsible for miR-196a underexpression in KF, we used a methylation-specific PCR method. Mature miR-196a derives from two pri-miRNAs: pri-miR-196a-1 (genomic region, chr17:46709852-46709921) and pri-miR-196a-2 (genomic region, chr12:54385522-54385631); genomic regions are based on the NCBI database (http://www.ncbi.nlm.nih.gov/). We then examined both promoter regions of these two pri-miRNAs. As previous studies have indicated that most human miRNA promoters are located around -1,000 bp upstream of mature miRNA (Saini *et al.*, 2008; Zhou *et al.*, 2007), primers designed within CpG island that are located on the putative promoter region were used (Hoffman *et al.*, 2009; Suzuki *et al.*, 2011). As shown in Figure 4a, unmethylated promoters were dominant for pri-miR-196a-1. On the other hand, methylation was remarkable for pri-miR-196a-2 (Figure 4b). However, there were no differences in the level of methylation status between KF and NF in both loci (Figure 4a and 4b). These data suggest that downregulation of the miR-196a expression in KF is not due to epigenetic regulation by aberrant methylation of their promoter regions. Other upstream unknown factors may be involved in this regulation.

In summary, the expression profiles of miRNA between KF and NF were apparently distinct. Since it has been demonstrated that each individual miRNA could have hundreds of mRNA targets, miRNAs that are differentially regulated in KF may play a variety of roles in keloid pathogenesis. miR-196a displayed the highest altered expression in KF compared with NF and regulated the expression of type I and III collagens, whose deposition is a major manifestation in keloid pathology. The mechanisms of the reduced expression of miRNA-196a still remain to be elucidated; however, miR-196a could be an attractive therapeutic target, since there have been attempts trying topical administration of RNA-based drugs (Bak and Mikkelsen, 2010; Ritprajak *et al.*, 2008; Takanashi *et al.*, 2009).

Materials and Methods

Tissue samples

Nine keloid tissue samples were obtained from eight different Japanese patients at the time of surgery, and diagnosis was confirmed by routine pathological examination. Normal skin tissue samples were obtained from nine different Japanese volunteers. All experiments were performed after obtaining approval of the ethical committee of Nagasaki University Hospital and adhered to the Helsinki Guidelines. Written informed consent was obtained from each individual. The sample profiles are summarized in Table 1.

Cell culture

Primary culture of dermal fibroblasts were established as previously described (Arakawa *et al.*, 1990). Explants were maintained in Dulbecco's modified Eagle's medium (DMEM)

supplemented with 10% heat-inactivated fetal bovine serum (FBS) and 1% (w/v) penicillin/streptomycin in 5% CO_2 humidified atmosphere at 37°C. Fibroblast obtained at the first culture for two weeks (at passage 0) were used in this study, except as indicated otherwise.

miRNA microarray

Total RNAs were extracted from KF and NF using a miRNeasy mini kit (QIAGEN, Tokyo, Japan) according to the manufacturer's instruction. Five hundred nanograms of the total RNAs were subjected to an Agilent miRNA microarray analysis service (Hokkaido System Science, Sapporo, Japan). Data analysis was done with GeneSpring GX software (Agilent Technology Japan, Tokyo, Japan). The array contained probes for 866 human and 89 viral miRNAs. Probes with "present call" flag in at least one sample in both groups were used for further data analyses (27 probes). Differences between groups were examined for statistical significance with unpaired t-test. p-value not exceeding 0.05 was considered statistically significant.

Real-time RT-PCR for miRNA

The quantitative real-time RT-PCR for miRNA was performed using TaqMan MicroRNA Assays (Applied Biosystems, Life Technologies Japan, Tokyo, Japan). Briefly, 10 ng of total RNA were reverse transcribed using a specific looped RT primer for each miRNA using a corresponding TaqMan MicroRNA Reverse Transcription kit (Applied Biosystems). The following amplification was performed using a corresponding TaqMan MicroRNA Assay Mix, TaqMan Universal PCR Master Mix and No AmpErase UNG (Applied Biosystems) in a Thermal Cycler Dice Real-time system (TaKaRa Bio, Ohtsu, Japan). RNU6B was used as an internal control. The cycle threshold value, which was determined

using second derivative, was used to calculate the normalized expression of the indicated miRNAs using Q-Gene software (Muller *et al.*, 2002).

Real-time RT-PCR for mRNA

Total RNA was extracted using ISOGEN reagent (NIPPON GENE, Tokyo, Japan) according to the manufacturer's instruction. One microgram of total RNA was reverse transcribed using a High capacity RNA-to-cDNA kit (Applied Biosystems). The following PCR amplification was carried out in a Thermal Cycler Dice Real-time system using SYBR Premix Ex Taq II (TaKaRa Bio). For each sample, the relative mRNA level was normalized by ribosomal RNA 18S. The following primer pairs were used: *COL1A1* sense, CGAAGACATCCCACCAATCAC and anti-sense, GATCGCACAACACCTTGCC; *COL1A2* sense, TGCCTAGCAACATGCCAATC and anti-sense, TCCTCTATCTCCGGCTGGG; *COL3A1* sense, TCCCACTATTATTTTGGCACAACA and anti-sense, TCATCGCAGAGA ACGACGGATCC; 18S sense, GTAACCCGTTGAACCCCATT and anti-sense, CCATCCAATCGGTAGTAGCG.

Western blot

To obtain secreted ECM proteins, culture media were collected and filtered with a 0.22 μm filter (MillexGV, Millipore, Bedford, MA). Protein concentration was determined with a Bichinonic Acid Assay kit (Sigma-Aldrich Japan, Tokyo, Japan). Equal amount of proteins (15 μg) were mixed in sample buffer containing 0.125 M Tris-HCl (pH6.8), 30% Glycerol, 35 μM sodium dodecyl sulfate, 60 μM dithiothreitol and bromphenol blue. After heated for 3 min at 99°C, the proteins were resolved by SDS-PAGE and transferred onto polyvinylidene difluoride membrane (Millipore) by semidry blotting. After incubation with appropriate primary antibody, the antigen-antibody complex was visualized using

horseradish peroxidase (HRP)-conjugated secondary antibody and the Chemi-Lumi One system (Nacalai Tesque, Kyoto, Japan). To enhance sensitivity, Can Get Signal reagent (TOYOBO, Osaka, Japan) was used. Detection was performed using a LAS3000 imaging system (FUJI film, Tokyo, Japan). Antibodies were obtained from the following sources: anti-fibronectin polyclonal from Santa Cruz Biotechnology (Santa Cruz, CA); anti-collagen type I polyclonal and anti-collagen type III polyclonal from Rockland Immunochemicals (Gilbertsville, PA); HRP-conjugated secondary anti-rabbit/mouse IgG from Cell Signaling Technology (Beverly, MA).

Transfection of Pre-miR/Anti-miR-196a

Cells were transfected with Pre-miR^{TM} miRNA Precursor Molecule for miR-196a (Pre-miR-196a), Anti-miR^{TM} miRNA Inhibitor for miR-196a (Anti-miR-196a), FAM-labeled Pre-miR^{TM} Scrambled Negative Control #1 or Anti-miR^{TM} Scrambled Negative Control #1 using Lipofectamine 2000 (Invitorogen, Life Technologies Japan, Tokyo, Japan) at the final concentration of 50 nM. All the above functional molecules were purchased from Applied Biosystems. Transfection efficiency was assessed using a fluorescence microscopy DM6000B (Leica Microsystems, Tokyo, Japan).

Luciferase reporter assay

The 3'UTRs containing the putative miRNA target regions of the *COL1A1* and *COL3A1* genes were amplified by PCR using fibroblast genomic DNA as a template. The following primer pairs were used: *COL1A1* sense, ATTCCACTCGAGCTCCCTCCATCCCAACCTGGC and anti-sense, GCCATAGTCGACATGTTTGGGTCATTTCCACATGCTT; *COL3A1* sense, ACAGCTCTCGAGACCAAACTCTATCTGAAATCCCAACA and anti-sense,

AGAATCGTCGACGAATTTTAATATGATATTTTATTATGGGTG. The sense and anti-sense primers carry the Xho I and Sal I sites at their 5'-ends, respectively. The obtainted DNA fragments were inserted into pmirGLO plasmid (Promega, Tokyo, Japan) to generate pmirGLO-COL1A1-3'UTR and pmirGLO-COL3A1-3'UTR. Fibroblasts were seeded on 96-well plates in DMEM supplemented with 10% FBS at a density of 1×10^4 cells/well. And they were transfected with 200 ng of the reporter plasmid together with Pre-miR-196a, Anti-miR-196a or Scrambled control. The Dual-Glo Luciferase Assay System (Promega) and a TD-20/20 luminometer (Turner Designs, Sunnyvale, CA) were used to analyze luciferase expression according to the manufacturer's protocol. *Firefly* luciferase activity was measured and normalized to *Renilla* luciferase activity to adjust for variations in transfection efficiency among experiments.

Methylation-specific PCR

DNA methylation patterns in the promoter region of the miR-196a-1 and miR-196a-2 genes were analyzed by methylation-specific PCR as previously described with minor modifications (Esteller *et al.*, 1999; Umetani *et al.*, 2005). Briefly, genomic DNA was isolated from cells using a QIAamp DNA Mini kit (QIAGEN). Bisulfite conversion was then carried out using an EpiTect Bisulfite kit (QIAGEN). Following PCR was done using ExTaq HS (TaKaRa Bio). The primer sequences are as described previously: for miR-196a-1 (Suzuki *et al.*, 2011) and for miR-196a-2 (Hoffman *et al.*, 2009). The thermal profile was: 95°C for 3 min; 40 cycles of 94°C for 30 s, 61°C (196a-1) or 49°C (196a-2) for 30 s and 72°C for 10 s. DNA from T98G (glioblastoma cell line) was treated with SssI methyltransferase (New England Biolabs, Beverly, MA) and used as a methylated control. DNA from T98G was amplified by a GenomiPhi V2 kit (GE Healthcare Bio-sciences, Piscataway, NJ) and used as an unmethylated control. PCR product was loaded onto a 3%

agarose gel, stained with ethidium bromide and visualized under ultraviolet illumination with a Bio-Doc-It (UVP, Cambridge, UK).

Statistical analysis

Difference between two related groups was examined for statistical significance with paired t-test, and two independent groups were examined with Mann-Whitney test. For more than two groups, one-way ANOVA followed by Tukey's post test was used. P-value not exceeding 0.05 was considered statistically significant. Data were analyzed with PRISM version 4 software (GraphPad Software, La Jolla, CA).

Conflict of Interest

The authors state no conflict of interest.

Acknowledgements

This work was supported in part by Global COE Program from the Ministry of Education, Culture, Sports, Science and Technology of Japan. We thank Ms. Mayuko Shimada for generating the luciferase plasmids.

References

Al-Attar A, Mess S, Thomassen JM, *et al.* (2006) Keloid pathogenesis and treatment. *Plast Reconstr Surg* 117:286-300.

Ala-Kokko L, Rintala A, Savolainen ER (1987) Collagen gene expression in keloids: analysis of collagen metabolism and type I, III, IV, and V procollagen mRNAs in keloid tissue and keloid fibroblast cultures. *J Invest Dermatol* 89:238-44.

Arakawa M, Hatamochi A, Takeda K, *et al.* (1990) Increased collagen synthesis accompanying elevated m-RNA levels in cultured Werner's syndrome fibroblasts. *J Invest Dermatol* 94:187-90.

Baek D, Villen J, Shin C, *et al.* (2008) The impact of microRNAs on protein output. *Nature* 455:64-71.

Bak RO, Mikkelsen JG (2010) Regulation of cytokines by small RNAs during skin inflammation. *J Biomed Sci* 17:53.

Bandres E, Agirre X, Bitarte N, *et al.* (2009) Epigenetic regulation of microRNA expression in colorectal cancer. *Int J Cancer* 125:2737-43.

Bartel DP (2004) MicroRNAs: genomics, biogenesis, mechanism, and function. *Cell* 116:281-97.

Bartel DP (2009) MicroRNAs: target recognition and regulatory functions. *Cell* 136:215-33.

Betel D, Wilson M, Gabow A, *et al.* (2008) The microRNA.org resource: targets and expression. *Nucleic Acids Res* 36:D149-53.

Brown BD, Naldini L (2009) Exploiting and antagonizing microRNA regulation for therapeutic and experimental applications. *Nat Rev Genet* 10:578-85.

Chau BN, Brenner DA (2011) What goes up must come down: the emerging role of microRNA in fibrosis. *Hepatology* 53:4-6.

Doench JG, Sharp PA (2004) Specificity of microRNA target selection in translational repression. *Genes Dev* 18:504-11.

Esquela-Kerscher A, Slack FJ (2006) Oncomirs - microRNAs with a role in cancer. *Nat Rev Cancer* 6:259-69.

Esteller M, Hamilton SR, Burger PC, *et al.* (1999) Inactivation of the DNA repair gene O6-methylguanine-DNA methyltransferase by promoter hypermethylation is a common event in primary human neoplasia. *Cancer Res* 59:793-7.

Feghali CA, Wright TM (1999) Identification of multiple, differentially expressed messenger RNAs in dermal fibroblasts from patients with systemic sclerosis. *Arthritis Rheum* 42:1451-7.

Hirth A, Skapenko A, Kinne RW, *et al.* (2002) Cytokine mRNA and protein expression in primary-culture and repeated-passage synovial fibroblasts from patients with rheumatoid arthritis. *Arthritis Res* 4:117-25.

Hoffman AE, Zheng T, Yi C, *et al.* (2009) microRNA miR-196a-2 and breast cancer: a genetic and epigenetic association study and functional analysis. *Cancer Res* 69:5970-7.

Jiang X, Tsitsiou E, Herrick SE, *et al.* (2010) MicroRNAs and the regulation of fibrosis. *FEBS J* 277:2015-21.

Kozaki K, Imoto I, Mogi S, *et al.* (2008) Exploration of tumor-suppressive microRNAs silenced by DNA hypermethylation in oral cancer. *Cancer Res* 68:2094-105.

Krek A, Grun D, Poy MN, *et al.* (2005) Combinatorial microRNA target predictions. *Nat Genet* 37:495-500.

Lewis BP, Burge CB, Bartel DP (2005) Conserved seed pairing, often flanked by adenosines, indicates that thousands of human genes are microRNA targets. *Cell* 120:15-20.

Lu M, Zhang Q, Deng M, *et al.* (2008) An analysis of human microRNA and disease associations. *PLoS One* 3:e3420.

Lujambio A, Ropero S, Ballestar E, *et al.* (2007) Genetic unmasking of an epigenetically silenced microRNA in human cancer cells. *Cancer Res* 67:1424-9.

Maurer B, Stanczyk J, Jungel A, *et al.* (2010) MicroRNA-29, a key regulator of collagen expression in systemic sclerosis. *Arthritis Rheum* 62:1733-43.

Muller PY, Janovjak H, Miserez AR, *et al.* (2002) Processing of gene expression data generated by quantitative real-time RT-PCR. *Biotechniques* 32:1372-4, 6, 8-9.

Niessen FB, Spauwen PH, Schalkwijk J, *et al.* (1999) On the nature of hypertrophic scars and keloids: a review. *Plast Reconstr Surg* 104:1435-58.

Ogawa T, Iizuka M, Sekiya Y, *et al.* (2010) Suppression of type I collagen production by microRNA-29b in cultured human stellate cells. *Biochem Biophys Res Commun* 391:316-21.

Ritprajak P, Hashiguchi M, Azuma M (2008) Topical application of cream-emulsified

CD86 siRNA ameliorates allergic skin disease by targeting cutaneous dendritic cells. *Mol Ther* 16:1323-30.

Roderburg C, Urban GW, Bettermann K, *et al.* (2011) Micro-RNA profiling reveals a role for miR-29 in human and murine liver fibrosis. *Hepatology* 53:209-18.

Saini HK, Enright AJ, Griffiths-Jones S (2008) Annotation of mammalian primary microRNAs. *BMC Genomics* 9:564.

Seifert O, Bayat A, Geffers R, *et al.* (2008) Identification of unique gene expression patterns within different lesional sites of keloids. *Wound Repair Regen* 16:254-65.

Seifert O, Mrowietz U (2009) Keloid scarring: bench and bedside. *Arch Dermatol Res* 301:259-72.

Selbach M, Schwanhausser B, Thierfelder N, *et al.* (2008) Widespread changes in protein synthesis induced by microRNAs. *Nature* 455:58-63.

Shih B, Bayat A (2010) Genetics of keloid scarring. *Arch Dermatol Res* 302:319-39.

Smith JC, Boone BE, Opalenik SR, *et al.* (2008) Gene profiling of keloid fibroblasts shows altered expression in multiple fibrosis-associated pathways. *J Invest Dermatol* 128:1298-310.

Suzuki H, Takatsuka S, Akashi H, *et al.* (2011) Genome-wide Profiling of Chromatin Signatures Reveals Epigenetic Regulation of MicroRNA Genes in Colorectal Cancer. *Cancer Res* 71:5646-58.

Syed F, Ahmadi E, Iqbal SA, *et al.* (2011) Fibroblasts from the growing margin of keloid scars produce higher levels of collagen I and III compared with intralesional and

extralesional sites: clinical implications for lesional site-directed therapy. *Br J Dermatol* 164:83-96.

Szulgit G, Rudolph R, Wandel A, *et al.* (2002) Alterations in fibroblast alpha1beta1 integrin collagen receptor expression in keloids and hypertrophic scars. *J Invest Dermatol* 118:409-15.

Takanashi M, Oikawa K, Sudo K, *et al.* (2009) Therapeutic silencing of an endogenous gene by siRNA cream in an arthritis model mouse. *Gene Ther* 16:982-9.

Thum T, Chau N, Bhat B, *et al.* (2011) Comparison of different miR-21 inhibitor chemistries in a cardiac disease model. *J Clin Invest* 121:461-2; author reply 2-3.

Thum T, Gross C, Fiedler J, *et al.* (2008) MicroRNA-21 contributes to myocardial disease by stimulating MAP kinase signalling in fibroblasts. *Nature* 456:980-4.

Tsai KW, Hu LY, Wu CW, *et al.* (2010) Epigenetic regulation of miR-196b expression in gastric cancer. *Genes Chromosomes Cancer* 49:969-80.

Umetani N, de Maat MF, Mori T, *et al.* (2005) Synthesis of universal unmethylated control DNA by nested whole genome amplification with phi29 DNA polymerase. *Biochem Biophys Res Commun* 329:219-23.

van Rooij E, Sutherland LB, Thatcher JE, *et al.* (2008) Dysregulation of microRNAs after myocardial infarction reveals a role of miR-29 in cardiac fibrosis. *Proc Natl Acad Sci U S A* 105:13027-32.

Yuan H, Kaneko T, Matsuo M (1996) Increased susceptibility of late passage human diploid fibroblasts to oxidative stress. *Exp Gerontol* 31:465-74.

Zhou X, Ruan J, Wang G, *et al.* (2007) Characterization and identification of microRNA core promoters in four model species. *PLoS Comput Biol* 3:e37.

Table 1. The profile of each sample for primary culture

		Sex	Age (years)	Biopsy site	Duration of the lesion (years)	etiology	previous treatment
Keloid							
*	KF 1	Female	22	Chest	10	Acne	topical corticosteroid, oral adminisitration of Tranilast
*	KF 2	Female	20	Chest	5	Acne	topical corticosteroid
*	KF 3	Female	15	Shoulder	7	Blister	topical corticosteroid
	KF 4	Felmale	22	Shoulder	10	Unkown	topical corticosteroid, oral adminisitration of Tranilast
	KF 5	Male	39	Shoulder	20	Post ope	resection and electron beam
	KF 6	Male	78	Chest	11	Post ope	-
	KF 7	Male	38	Chest	20	Acne	-
	KF 8	Male	16	Shoulder	2	Blister	-
	KF 9	Male	63	Chest	3	Post ope	topical corticosteroid, oral adminisitration of Tranilast
Normal							
*	NF 1	Female	16	Chest	-	-	-
*	NF 2	male	82	Thigh	-	-	-
*	NF 3	Female	36	Thigh	-	-	-
	NF 4	Male	75	Chest	-	-	-
	NF 5	Male	62	Abdomen	-	-	-
	NF 6	Male	73	Palpebra	-	-	-
	NF 7	Male	54	Thigh	-	-	-
	NF 8	Female	60	Abdomen	-	-	-
	NF 9	Female	62	Abdomen	-	-	-

* Samples used for Agilent miRNA microarray

Table 2. Fold change of miRNAs expression

miRNA	Fold change (KF/NF)
hsa-miR-142-3p	9.856
hsa-miR-1249	4.068
hsa-miR-136	3.978
hsa-miR-376a*	2.464
hsa-miR-140-5p	1.968
hsa-miR-193a-3p	1.933
hsa-miR-1234	1.333
hsa-miR-23a	0.634
hsa-miR-574-3p	0.628
hsa-let-7d	0.600
hsa-miR-331-3p	0.578
hsa-miR-24	0.553
hsa-let-7a	0.545
hsa-miR-30e*	0.543
hsa-miR-93	0.541
hsa-let-7f	0.540
hsa-miR-98	0.508
hsa-miR-31*	0.433
hsa-miR-31	0.425
hsa-miR-224	0.373
hsa-miR-30a*	0.362
hsa-miR-769-5p	0.331
hsa-miR-595	0.290
hsa-miR-196b	0.246
hsa-miR-452	0.188
hsa-miR-182	0.169
hsa-miR-196a	0.093

Figure legends

Figure 1 miRNA expression kinetics in different passages of KF and NF.

TaqMan real-time quantitative RT-PCR assay was performed for miR-142-3p and miR-196a in KF and NF at passage 0 and 2 using four samples each. (a) miR-142-3p expression kinetics. (b) miR-196a expression kinetics. Difference between passage 0 and 2 was examined for statistical significance with paired t-test (*p=0.0245), and difference between KF and NF was examined with Mann-Whitney test (**p<0.03).

Figure 2 TaqMan real-time quantitative RT-PCR for miR-142-3p and miR-196a in KF and NF at passage 0 using nine samples each.

(a) miR-142-3p was overexpressed (*p=0.0005) and (b) miR-196a was underexpressed (*p=0.0056) in KF compared with NF. The p-values were obtained by Mann-Whitney test. Horizontal bar shows median.

Figure 3 Functional analysis of miR-196a.

(a) After transfection of Pre-miR-196a, the level of miR-196a was confirmed by TaqMan real-time quantitative RT-PCR assay. *p<0.001 vs. others. The p-value was obtained by one-way ANOVA followed by Tukey's post test. (b) Indicated cells were transfected with Pre-miR-196a, Anti-miR-196a or scrambled control. Seventy-two hours after the transfection, cultured media (ECM) were analyzed by western blot. Fibronectin was used as a loading control. The migration positions of indicated procollagens and molecular weight (MW) marker are shown. Similar results were obtained using three different NF/KF lines. Pro I: procollagen α1(I)/α2(I), Processed I: pC/pN-collagen α1(I)/α2(I). Pro III: procollagen α1(III), Processed III: pC/pN-collagen α1(III). (c, d and e) Activity of luciferase reporter containing the 3'UTR regions of *COL1A1* or *COL3A1*. (c) Relative luciferase activity in KF vs. NF using nine samples

each. Cells were transfected with pmirGLO-COL1A1-3'UTR or pmirGLO-COL3A1-3'UTR and incubated for 24 hr. Luciferase activity was measured as described in Materials and Methods. Difference between KF and NF was examined for statistical significance with Mann-Whitney test. Horizontal bar shows median. (d and e) NF were co-transfected wtih the reporter plasmids and (d) Pre-miR-196a or (e) Anti-miR-196a. Twenty-four hours after the transfection, luciferase activity was measured. Bar shows mean ± SD of three independent experiments. The p-values were obtained by Mann-Whitney test.

Figure 4 Methylation status of the miR-196a promoters in KF and NF.

Genomic DNA was extracted and analyzed by methylation-specific PCR. (a) miR-196a-1. (b) miR-196a-2. Methylated control, unmethylated control and template-free negative control were also included. M: methylated, U: unmethylated.

Figure 1

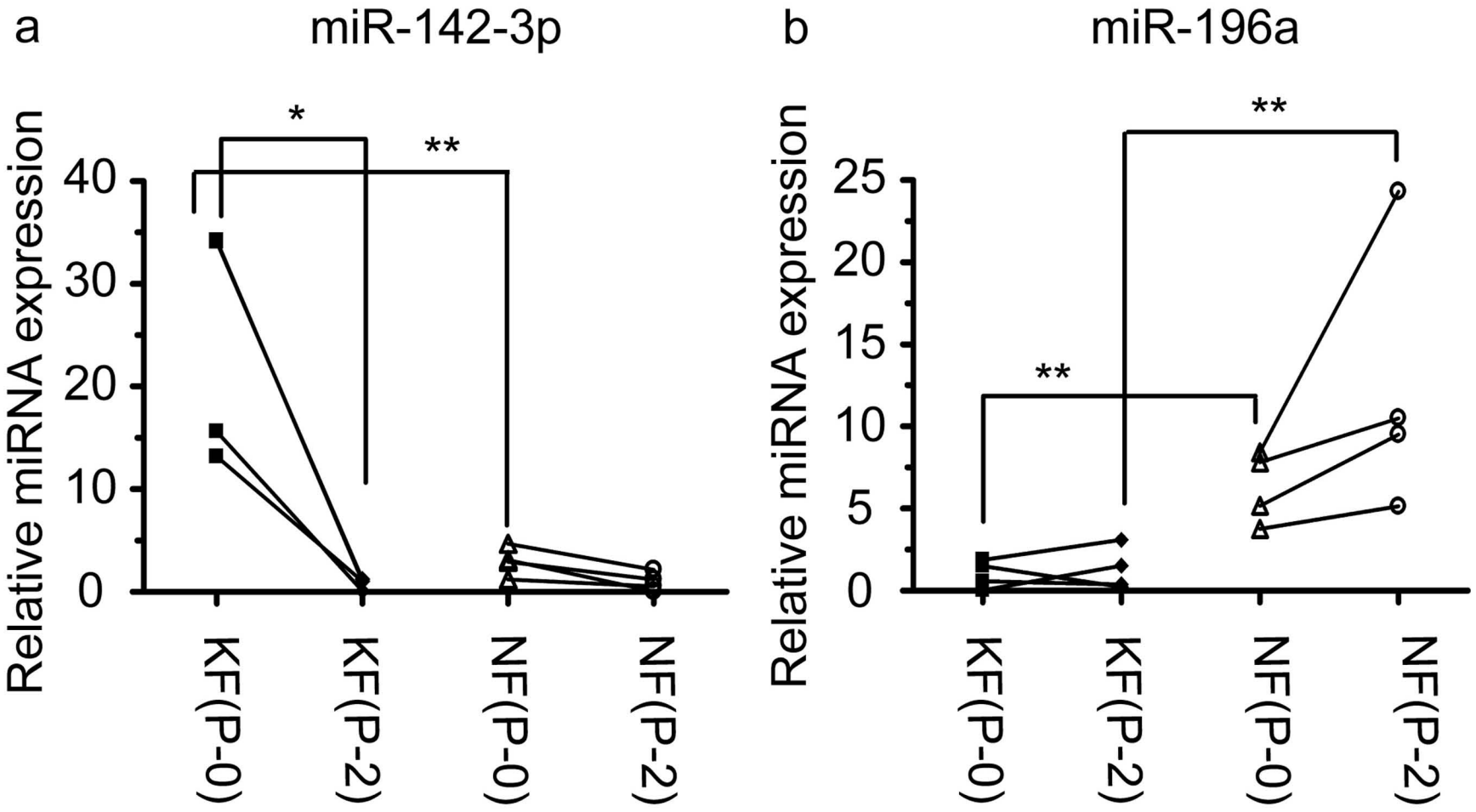
a
miR-142-3p
Relative miRNA expression
40
30
20
10
0
*
**
KF(P-0)
KF(P-2)
NF(P-0)
NF(P-2)
b
miR-196a
Relative miRNA expression
25
20
15
10
5
0
**
**
KF(P-0)
KF(P-2)
NF(P-0)
NF(P-2)

Figure 2

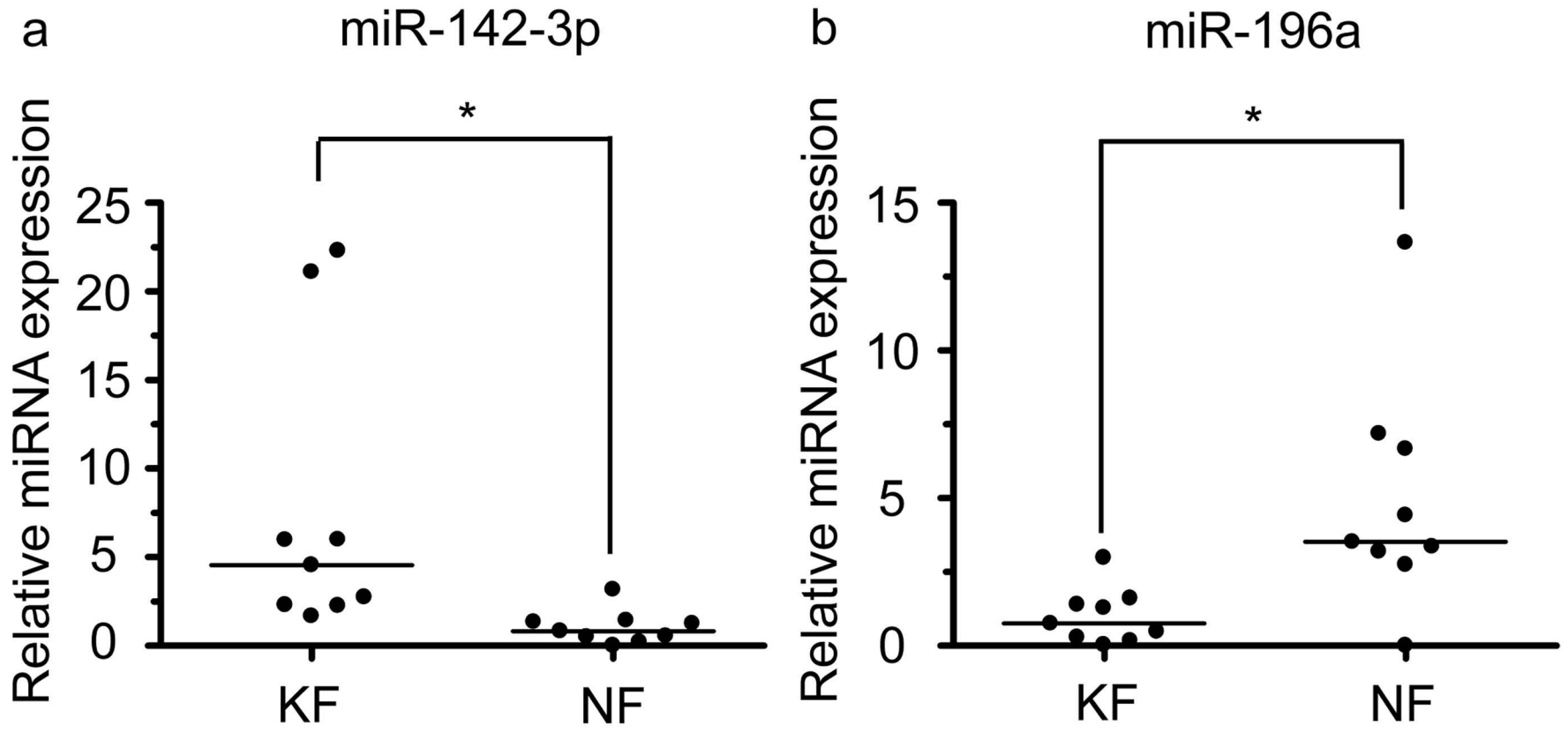
a
miR-142-3p
Relative miRNA expression
25
20
15
10
5
0
*
KF
NF
b
miR-196a
Relative miRNA expression
15
10
5
0
*
KF
NF

Figure 3

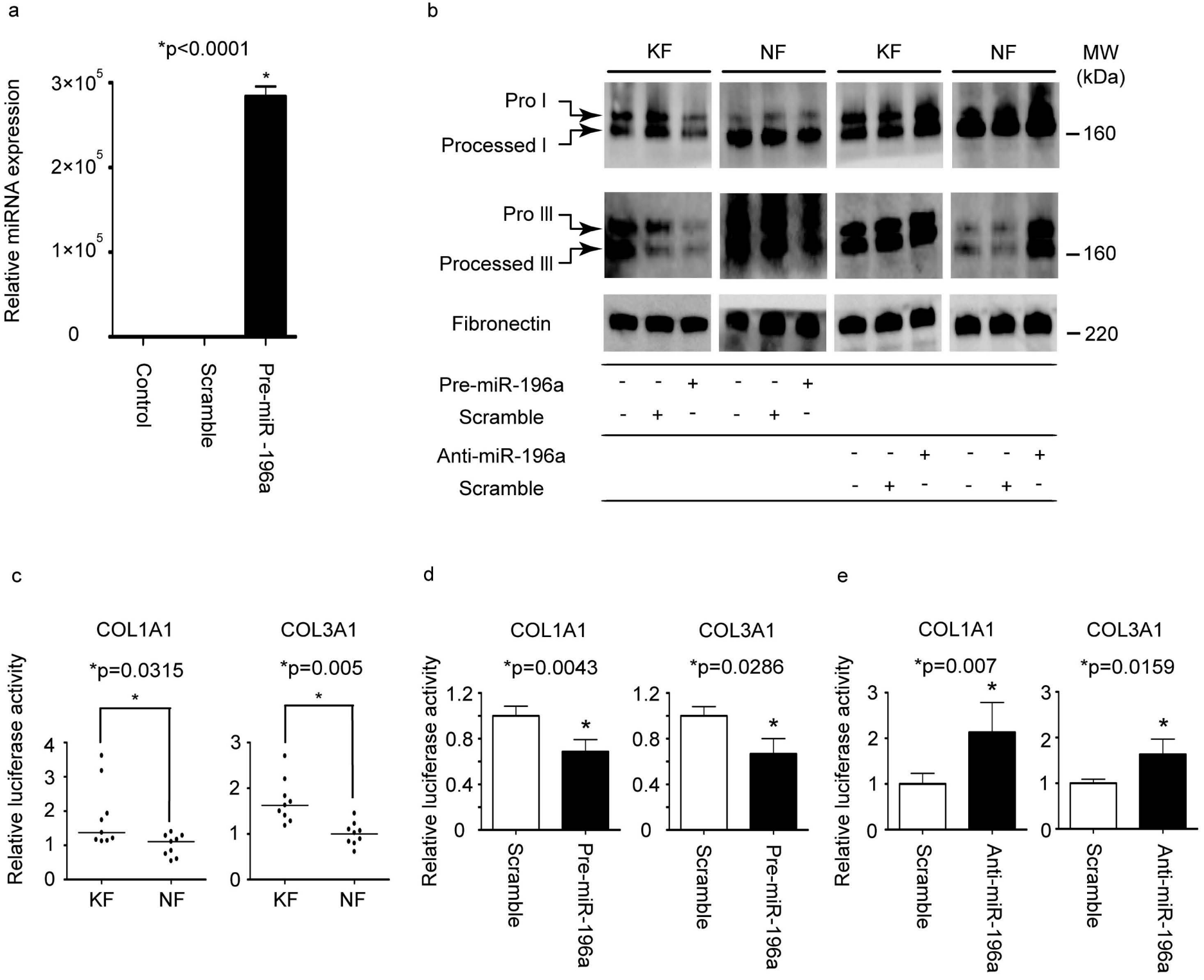
a
*p<0.0001
Relative miRNA expression
3×10^5
2×10^5
1×10^5
0
*
Control
Scramble
Pre-miR -196a
b
KF
NF
KF
NF
MW (kDa)
Pro I
Processed I
160
Pro III
Processed III
160
Fibronectin
220
Pre-miR-196a
Scramble
Anti-miR-196a
Scramble
c
COL1A1
*p=0.0315
COL3A1
*p=0.005
Relative luciferase activity
KF
NF
KF
NF
d
COL1A1
*p=0.0043
COL3A1
*p=0.0286
Relative luciferase activity
Scramble
Pre-miR-196a
Scramble
Pre-miR-196a
e
COL1A1
*p=0.007
COL3A1
*p=0.0159
Relative luciferase activity
Scramble
Anti-miR-196a
Scramble
Anti-miR-196a

Figure 4

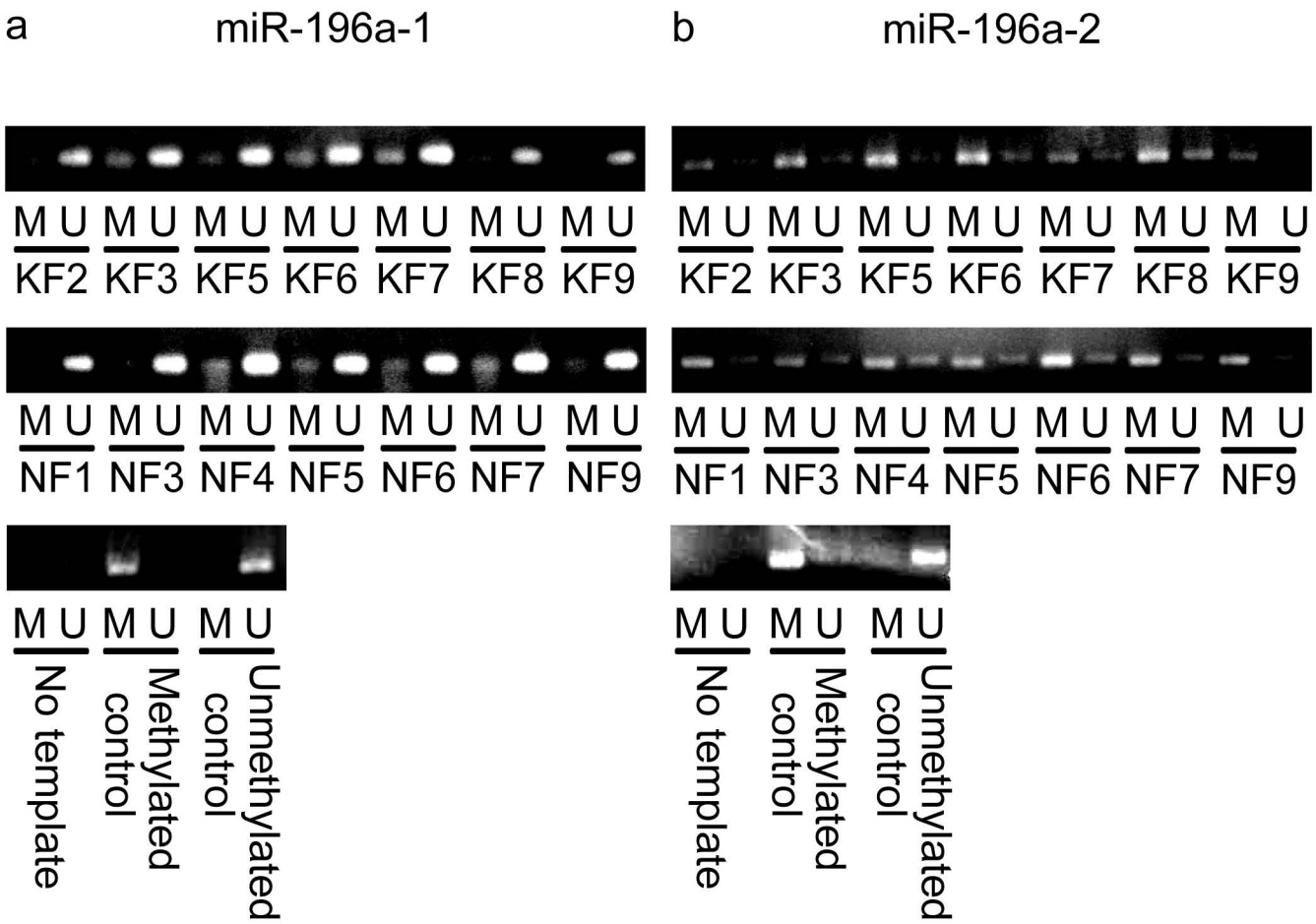
a
miR-196a-1
b
miR-196a-2
M U
KF2 KF3 KF5 KF6 KF7 KF8 KF9
NF1 NF3 NF4 NF5 NF6 NF7 NF9
No template
Methylated control
Unmethylated control

Supplementary Material

Supplemental figure legends

Figure S1

Possible target mRNAs of each miRNA. Venn diagrams of the number of predicted target miRNAs in indicated web-based database are shown. 70 and 47 genes were commonly shared in miR-142-3p and miR-196a, respectively.

Figure S2

Relative mRNA expression of collagens in KF and NF. Total RNA extracted from KF and NF at passage 0 was subjected to real-time RT-PCR. Difference between KF and NF was examined for statistical significance with Mann Whitney test. Each bar indicates mean ± SD of nine samples. *$p<0.03$ vs. NF.

Figure S3

Predicted miRNA binding sites in the 3'UTRs of *COL1A1, COL1A2* and *COL3A1* mRNAs based on TargetScan Human Release 5.1 (http://www.targetscan.org/). The complementarity between the target sites and the miR-196a seed region (2-8 nucleotides of the 5'UTR of miR-196a). Predicted consequential pairing of target region are 787-793 of *COL1A1* 3'UTR, 377-383 of *COL1A2* 3'UTR and 407-413 of *COL3A1* 3'UTR.

Figure S1

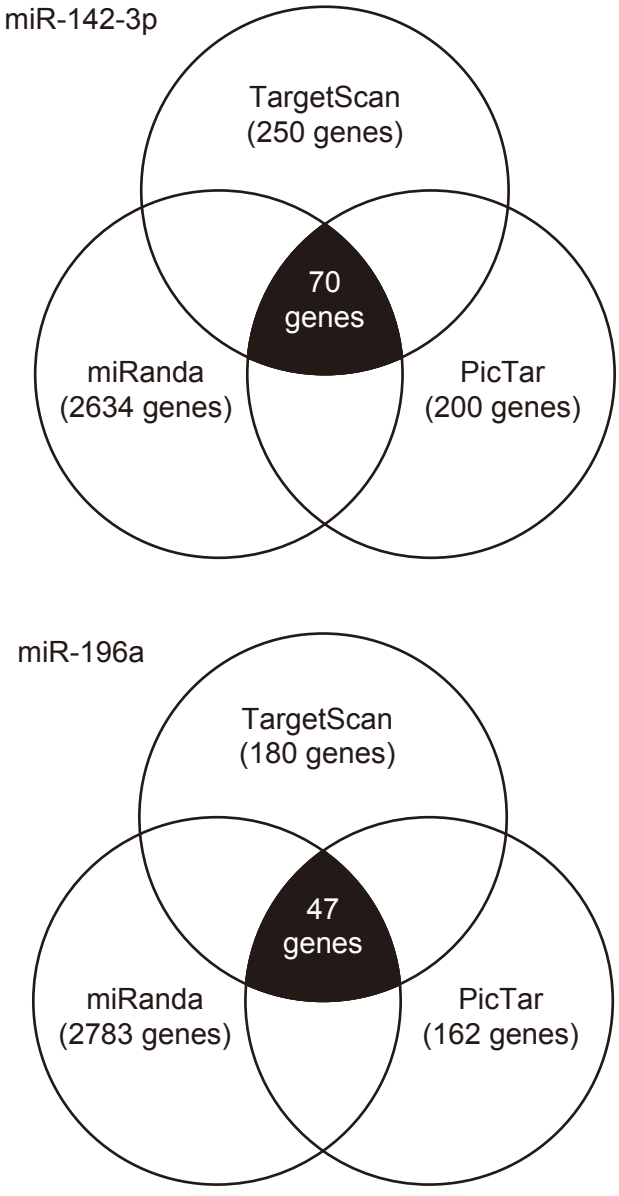
miR-142-3p
TargetScan
(250 genes)
70
genes
miRanda
(2634 genes)
PicTar
(200 genes)
miR-196a
TargetScan
(180 genes)
47
genes
miRanda
(2783 genes)
PicTar
(162 genes)

Figure S2

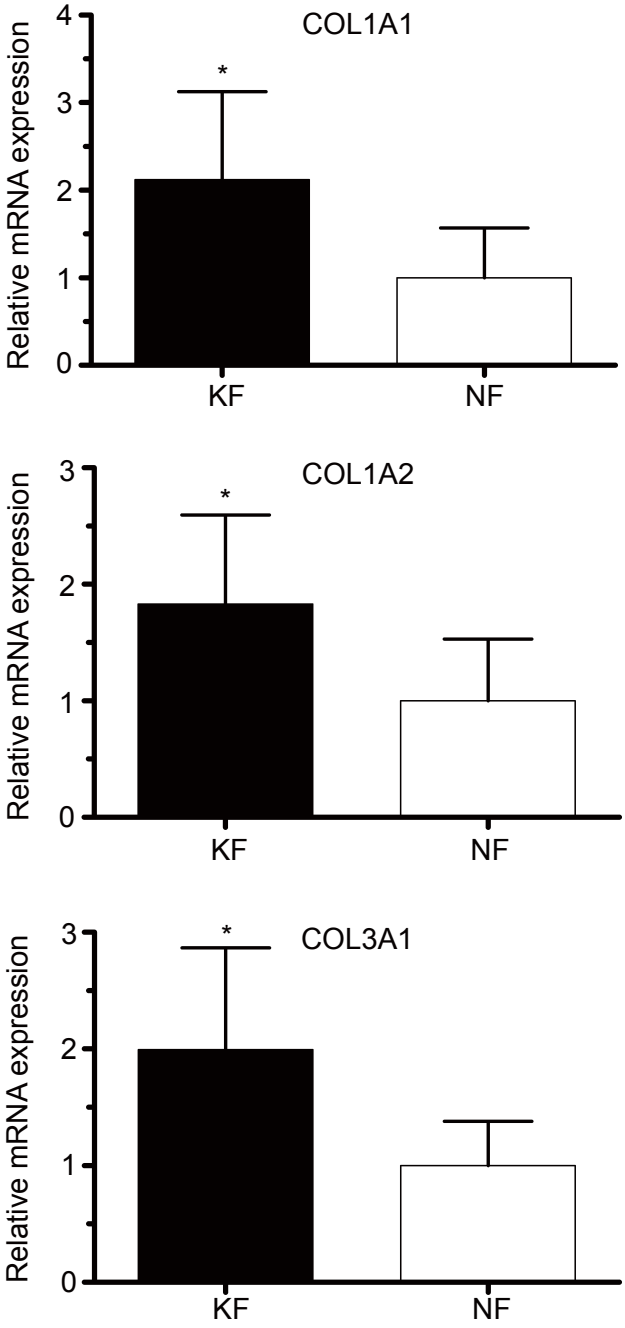
COL1A1
Relative mRNA expression
4
3
2
1
0
*
KF
NF
COL1A2
Relative mRNA expression
3
2
1
0
*
KF
NF
COL3A1
Relative mRNA expression
3
2
1
0
*
KF
NF

Figure S3

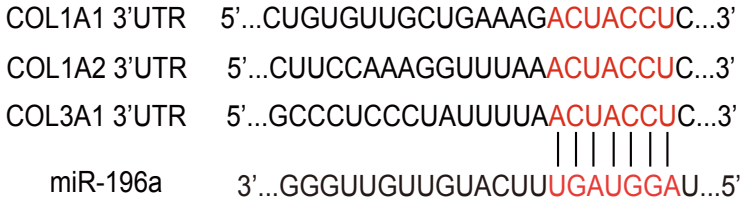
COL1A1 3'UTR 5'...CUGUGUUGCUGAAAGACUACCUC...3'
COL1A2 3'UTR 5'...CUUCCAAAGGUUUAAACUACCUC...3'
COL3A1 3'UTR 5'...GCCCUCCCUAUUUUAACUACCUC...3'
miR-196a 3'...GGGUUGUUGUACUUUGAUGGAU...5'

Table S1. Predicted target of miR-142-3p

Gene symbol	Gene discription	human Refseq Id	PicTar	TargetScan		miRanda
			PicTar score	total context score	P_{CT}	mirSVR score
ACBD5	acyl-Coenzyme A binding domain containing 5	NM_145698	3.31	-0.21	0.65	-0.1868
ADAMTS3	ADAM metallopeptidase with thrombospondin type 1 motif, 3	NM_014243	1.98	-0.3	0.78	-0.7251
ADCY9	adenylate cyclase 9	NM_001116	1.55	-0.17	0.81	-0.59
AKT1S1	AKT1 substrate 1 (proline-rich)	NM_032375	7.77	-0.14	0.78	-0.2896
ANK3	ankyrin 3, node of Ranvier (ankyrin G)	NM_020987	2.23	-0.4	0.43	-1.2813
ARNTL	aryl hydrocarbon receptor nuclear translocator-like	NM_001178	7.29	-0.47	0.74	-1.2323
ATF7IP	activating transcription factor 7 interacting protein	NM_018179	3.44	-0.49	0.86	-1.2933
BACH1	BTB and CNC homology 1, basic leucine zipper transcription factor 1	NM_001186	3.58	-0.25	0.83	-0.6607
BCLAF1	BCL2-associated transcription factor 1	NM_014739	1.97	-0.33	0.8	-0.3974
BTBD7	BTB (POZ) domain containing 7	NM_001002860	2.78	-0.25	0.81	-0.5677
C1orf9	chromosome 1 open reading frame 9	NM_014283	2.87	-0.36	0.72	-1.0981
C9orf72	chromosome 9 open reading frame 72	NM_018325	2.55	-0.43	0.87	-0.7701
CCNT2	cyclin T2	NM_058241	2.46	-0.42	0.24	-1.2744
CFL2	cofilin 2 (muscle)	NM_138638	6.28	-0.35	0.57	-0.781
CLTA	clathrin, light chain (Lca)	NM_007096	4.13	-0.39	0.48	-1.2907

COL24A1	collagen, type XXIV, alpha 1	NM_152890	2.7	-0.17	0.73	-1.0358
COPG	coatomer protein complex, subunit gamma	NM_016128	3.17	-0.16	0.78	-0.1464
COPS7A	COP9 constitutive photomorphogenic homolog subunit 7A (Arabidopsis)	NM_016319	2.85	-0.29	0.38	-0.8042
CPEB2	cytoplasmic polyadenylation element binding protein 2	NM_182646	1.82	-0.42	0.74	-1.0289
CRK	v-crk sarcoma virus CT10 oncogene homolog (avian)	NM_016823	2.64	-0.22	0.8	-1.0232
CRTAM	cytotoxic and regulatory T cell molecule	NM_019604	2.44	-0.18	0.82	-0.4982
DIRC2	disrupted in renal carcinoma 2	NM_032839	3.3	-0.49	0.84	-1.0169
DMTF1	cyclin D binding myb-like transcription factor 1	NM_021145	2.52	-0.2	0.7	-0.1807
EML4	echinoderm microtubule associated protein like 4	NM_019063	5.49	-0.42	0.93	-0.7027
ERG	v-ets erythroblastosis virus E26 oncogene homolog (avian)	NM_004449	2.43	-0.23	0.81	-0.9624
FKBP1A	FK506 binding protein 1A, 12kDa	NM_000801	5.46	-0.19	0.25	-0.2441
FMNL2	formin-like 2	NM_052905	3.71	-0.49	0.66	-1.3108
GFI1	growth factor independent 1 transcription repressor	NM_005263	2.41	-0.31	0.78	-0.1672
GNAQ	guanine nucleotide binding protein (G protein), q polypeptide	NM_002072	2.54	-0.33	0.82	-0.7558
GNB2	guanine nucleotide binding protein (G protein), beta polypeptide 2	NM_005273	4.09	-0.14	0.79	-0.2118
GTF2A1	general transcription factor IIA, 1, 19/37kDa	NM_015859	4.04	-0.16	0.76	-0.916
HECTD1	HECT domain containing 1	NM_015382	2.97	-0.37	0.84	-1.1872

HMGA2	high mobility group AT-hook 2	NM_003483	6.12	-0.34	0.64	-0.365
HMGB1	high-mobility group box 1	NM_002128	2.65	-0.22	0.83	-0.5721
INPP5A	inositol polyphosphate-5-phosphatase, 40kDa	NM_005539	2.29	-0.4	0.86	-0.9714
IRAK1	interleukin-1 receptor-associated kinase 1	NM_001569	2.93	-0.27	0.85	-0.1851
ITGAV	integrin, alpha V (vitronectin receptor, alpha polypeptide, antigen CD51)	NM_002210	1.66	-0.47	0.87	-0.9501
ITPKB	inositol 1,4,5-trisphosphate 3-kinase B	NM_002221	1.76	-0.12	0.77	-0.6009
LLGL2	lethal giant larvae homolog 2 (Drosophila)	NM_004524	4.21	N/A	0.82	-0.2197
LRRC1	leucine rich repeat containing 1	NM_018214	1.84	-0.38	0.83	-0.8925
MAP3K11	mitogen-activated protein kinase kinase kinase 11	NM_002419	3.51	-0.29	0.86	-0.6318
MARCKS	myristoylated alanine-rich protein kinase C substrate	NM_002356	2.59	-0.36	0.87	-0.6576
MARK3	MAP/microtubule affinity-regulating kinase 3	NM_002376	3.69	-0.17	0.63	-0.1626
PTPN23	protein tyrosine phosphatase, non-receptor type 23	NM_015466	4.34	-0.39	0.84	-0.7405
PUM1	pumilio homolog 1 (Drosophila)	NM_014676	2.31	-0.42	0.42	-1.1322
RAB1A	RAB1A, member RAS oncogene family	NM_004161	2.48	-0.17	0.67	-0.1344
RAB40C	RAB40C, member RAS oncogene family	NM_021168	3.01	-0.1	0.74	-0.1532
RAC1	ras-related C3 botulinum toxin substrate 1 (rho family, small GTP binding protein Rac1)	NM_198829	3.37	-0.47	0.74	-1.016
RARG	retinoic acid receptor, gamma	NM_000966	2.92	-0.21	0.84	-0.5929

RERE	arginine-glutamic acid dipeptide (RE) repeats	NM_012102	1.94	-0.29	0.83	-0.3051
RGL2	ral guanine nucleotide dissociation stimulator-like 2	NM_004761	3.43	-0.3	0.79	-1.1092
RLF	rearranged L-myc fusion	NM_012421	4.28	-0.46	0.75	-1.1976
ROCK2	Rho-associated, coiled-coil containing protein kinase 2	NM_004850	5.88	-0.4	0.74	-0.3735
SLC37A3	solute carrier family 37 (glycerol-3-phosphate transporter), member 3	NM_032295	5.35	-0.7	0.84	-0.3953
SLCO4C1	solute carrier organic anion transporter family, member 4C1	NM_180991	1.95	-0.22	0.81	-0.5692
SMG1	PI-3-kinase-related kinase SMG-1	NM_014006	1.97	-0.36	0.79	-0.6186
STAM	signal transducing adaptor molecule (SH3 domain and ITAM motif) 1	NM_003473	2.76	-0.5	0.73	-1.2961
STRN3	striatin, calmodulin binding protein 3	NM_014574	2.52	-0.36	0.7	-0.7863
STX12	syntaxin 12	NM_177424	2.34	-0.36	0.77	-0.7967
TAOK1	TAO kinase 1	NM_020791	2.46	-0.34	0.86	-1.0159
TARDBP	TAR DNA binding protein	NM_007375	2.2	-0.37	0.67	-0.5935
TFG	TRK-fused gene	NM_006070	3.65	-0.24	0.6	-0.98
TIPARP	TCDD-inducible poly(ADP-ribose) polymerase	NM_015508	2.31	-0.25	0.79	-1.1267
TP53INP2	tumor protein p53 inducible nuclear protein 2	NM_021202	2.38	-0.16	0.71	-0.5312
UTY	ubiquitously transcribed tetratricopeptide repeat gene, Y-linked	NM_007125	2.76	-0.28	0.83	-1.0636
VAMP3	vesicle-associated membrane protein 3 (cellubrevin)	NM_004781	2.1	-0.23	0.81	-0.9236

VPS24	vacuolar protein sorting 24 homolog (S. cerevisiae)	NM_016079	2.79	-0.12	0.7	-0.1824
XPO1	exportin 1 (CRM1 homolog, yeast)	NM_003400	3.17	-0.31	0.8	-1.2471
ZFP91	zinc finger protein 91 homolog (mouse)	NM_053023	1.44	-0.11	0.62	-0.4678
ZNF217	zinc finger protein 217	NM_006526	2.51	-0.4	0.86	-0.8279

Table S2. Predicted target of miR-196a

Gene symbol	Gene discription	human Refseq Id	PicTar	TargetScan		miRanda
			PicTar score	total context score	P_{CT}	mirSVR score
ABCB9	ATP-binding cassette, sub-family B (MDR/TAP), member 9	NM_203444	2.7	-0.21	0.83	-0.1742
ADCY9	adenylate cyclase 9	NM_001116	1.37	-0.11	0.7	-0.1624
AQP4	aquaporin 4	NM_001650	1.93	-0.49	0.51	-0.2265
BACH1	BTB and CNC homology 1, basic leucine zipper transcription factor 1	NM_001186	2.44	-0.28	0.9	-0.4524
C20orf160	chromosome 20 open reading frame 160	NM_080625	2.84	-0.11	0.81	-0.1404
CBFA2T3	core-binding factor, runt domain, alpha subunit 2; translocated to, 3	NM_175931	2.63	-0.22	0.88	-0.4063
CCNJ	cyclin J	NM_019084	5.08	-0.45	0.84	-0.8718
CDKN1B	cyclin-dependent kinase inhibitor 1B (p27, Kip1)	NM_004064	2.72	-0.27	0.32	-1.1649
CDYL	chromodomain protein, Y-like	NM_004824	2.25	-0.33	0.63	-1.258
COL1A1	collagen, type I, alpha 1	NM_000088	1.91	-0.11	0.65	-0.2443
COL1A2	collagen, type I, alpha 2	NM_000089	2.53	-0.27	0.61	-1.1474
COL24A1	collagen, type XXIV, alpha 1	NM_152890	2.54	-0.12	0.58	-0.407
COL3A1	collagen, type III, alpha 1	NM_000090	2.31	-0.22	0.7	-0.9361
CPD	carboxypeptidase D	NM_001304	3.09	-0.38	0.84	-0.1389
EPC2	enhancer of polycomb homolog 2 (Drosophila)	NM_015630	2.96	-0.26	0.72	-1.2478

EPHA7	EPH receptor A7	NM_004440	1.97	-0.31	0.68	-0.7272
EPS15	epidermal growth factor receptor pathway substrate 15	NM_001981	2.24	-0.26	0.73	-0.6704
GAN	giant axonal neuropathy (gigaxonin)	NM_022041	3.83	-0.37	0.75	-0.7247
GATA6	GATA binding protein 6	NM_005257	2.25	-0.41	< 0.1	-1.2609
GGA3	golgi associated, gamma adaptin ear containing, ARF binding protein 3	NM_014001	3.78	-0.06	0.75	-0.2636
HAND1	heart and neural crest derivatives expressed 1	NM_004821	3.57	-0.45	0.65	-1.2632
HMGA2	high mobility group AT-hook 2	NM_003483	4.32	-0.42	0.82	-0.6059
HOXA5	homeobox A5	NM_019102	3.25	-0.47	0.61	-1.3565
HOXB6	homeobox B6	NM_156037	3.22	-0.38	0.65	-1.0685
HOXB7	homeobox B7	NM_004502	3.21	-0.49	0.65	-1.2444
HOXC8	homeobox C8	NM_022658	12.74	-1.31	> 0.99	-0.9864
ING5	inhibitor of growth family, member 5	NM_032329	2.17	-0.25	0.85	-0.3779
LRP1B	low density lipoprotein-related protein 1B (deleted in tumors)	NM_018557	2.17	-0.45	0.64	-1.2683
LRRTM3	leucine rich repeat transmembrane neuronal 3	NM_178011	2.22	-0.17	0.42	-0.1018
MAP4K3	mitogen-activated protein kinase kinase kinase kinase 3	NM_003618	2.8	-0.29	0.74	-1.2638
NRK	Nik related kinase	NM_198465	1.6	-0.14	0.61	-0.5758
OSMR	oncostatin M receptor	NM_003999	3.26	-0.21	0.53	-0.1379

PBX3	pre-B-cell leukemia homeobox 3	NM_006195	2.28	-0.19	0.74	-0.9153
PDGFRA	platelet-derived growth factor receptor, alpha polypeptide	NM_006206	1.56	-0.22	< 0.1	-0.411
PPP1R16B	protein phosphatase 1, regulatory (inhibitor) subunit 16B	NM_015568	1.2	-0.06	0.84	-0.187
RAD23B	RAD23 homolog B (S. cerevisiae)	NM_002874	2.07	-0.16	0.37	-0.1167
RANBP2	RAN binding protein 2	NM_006267	3.06	-0.14	0.79	-0.4415
RIOK3	RIO kinase 3 (yeast)	NM_003831	2.43	-0.2	0.85	-0.3857
SCHIP1	schwannomin interacting protein 1	NM_014575	3.37	-0.22	0.53	-1.0535
SLC31A1	solute carrier family 31 (copper transporters), member 1	NM_001859	2.36	-0.12	0.88	-0.3982
SLC9A6	solute carrier family 9 (sodium/hydrogen exchanger), member 6	NM_006359	4.18	-0.95	0.69	-1.1135
SMARCC1	SWI/SNF related, matrix associated, actin dependent regulator of chromatin, subfamily	NM_003074	2.89	-0.14	0.71	-0.1382
SOCS4	suppressor of cytokine signaling 4	NM_080867	2.19	-0.21	0.5	-0.1362
UHRF2	ubiquitin-like, containing PHD and RING finger domains, 2	NM_152896	2.95	-0.18	0.5	-0.2855
USP15	ubiquitin specific peptidase 15	NM_006313	2.22	-0.19	0.62	-0.5468
ZDHHC21	zinc finger, DHHC-type containing 21	NM_178566	2.28	-0.33	0.38	-0.8589
ZMYND11	zinc finger, MYND domain containing 11	NM_006624	6.56	-0.62	0.68	-1.0967